Journal of Nuclear Materials 392 (2009) 55–62

Contents lists available at ScienceDirect

Journal of Nuclear Materials

journal homepage: www.elsevier.com/locate/jnucmat

Deposition of RuO_4 on various surfaces in a nuclear reactor containment

Joachim Holm [a,*], Henrik Glänneskog [b], Christian Ekberg [a]

[a] Department of Nuclear Chemistry, Chalmers University of Technology, Se-412 96 Gothenburg, Sweden
[b] Ringhals AB, SE-430 22, Väröbacka, Sweden

ARTICLE INFO

Article history:
Received 9 December 2008
Accepted 12 March 2009

ABSTRACT

During a severe nuclear reactor accident with air ingress, ruthenium can be released from the nuclear fuel in the form of ruthenium tetroxide. Hence, it is important to investigate how the reactor containment is able to reduce the source term of ruthenium. The aim of this work was to investigate the deposition of gaseous ruthenium tetroxide on aluminium, copper and zinc, which all appear in relatively large amounts in reactor containment. The experiments show that ruthenium tetroxide is deposited on all the metal surfaces, especially on the copper and zinc surfaces. A large deposition of ruthenium tetroxide also appeared on the relatively inert glass surfaces in the experimental set-ups. The analyses of the different surfaces, with several analytical methods, showed that the form of deposited ruthenium was mainly ruthenium dioxide.

1. Introduction

During normal operation in a nuclear power plant, relatively high concentrations of ruthenium are formed by fission of uranium. Calculations made by Wright [1] show that about 330 kg of ruthenium are formed in the nuclear fuel in a boiling water reactor (BWR) at the end-of-cycle equilibrium core. This can be compared to the amounts of iodine and caesium that are formed, 30 and 430 kg, respectively. The amount of ruthenium in fuel increases with burn-up but decreases with ^{235}U enrichment [2]. The build up of ruthenium in the fuel is also in larger extent in MOX-fuel, due to higher fission yield of ruthenium for ^{239}Pu than ^{235}U. The radiotoxicity of ruthenium originates essentially from the two nuclides ^{103}Ru ($t_{½} \approx 40$ d) and ^{106}Ru ($t_{½} \approx 1$ y); thus ruthenium is radiologically important in both a short and a long perspective.

Ruthenium oxides may be formed in the reactor vessel during a severe accident with air ingress [3]. Events leading to air ingress occur during the late phase of a severe accident. Ruthenium oxides such as RuO_3 and more particularly RuO_4 are considerably volatile and can consequently be released from the reactor fuel and be transported through the reactor coolant system (RCS) and finally reach the containment. There are two main categories of air ingress to the reactor fuel:

(1) a melt-through scenario;
(2) a shutdown sequence with an open vessel lid.

The most probable scenario of an air ingress accident in a BWR is during the shutdown cycle with an open reactor lid. Since the atmosphere in the containment contains only a few percent oxygen during normal operation, it is not probable that significant amounts of oxygen can enter via openings in the reactor vessel created by melt-through. However, during a shutdown cycle with an open reactor lid and higher amounts of oxygen in the containment, a severe accident with air ingress can occur, leading to ruthenium oxidation.

The temperature in the containment under severe accident conditions will be relatively low, below 150 °C. The gaseous oxides $RuO(g)$, $RuO_2(g)$ and $RuO_3(g)$ are not thermodynamically stable under temperatures below 1000 °C and will probably not reach the containment [4]. Hence this study concentrated on the behaviour of gaseous RuO_4 in a BWR containment environment.

A BWR containment has many different surfaces, such as metals, painted concrete and cables, which can interact with gaseous RuO_4 and other volatile fission products. Deposition of gaseous RuO_4 on stainless steel surfaces is reported in the literature [5–7]. The authors [5,6] also report reduction of deposited RuO_4 to $RuO_2(s)$, through Eq. (1), on stainless steel surfaces. Mun et al. presented results that indicate that hydroxylized Ru(IV), $RuO(OH)_2$, is formed when gaseous ruthenium tetroxide is deposited on stainless steel and painted substrates [7]. However, other researchers have reported deposition of RuO_3 [8] and even RuO_4 [9] on metal surfaces such as stainless steel, after staining of $RuO_4(g)$ on the surfaces.

$$RuO_4(g) \rightarrow RuO_2(s) + O_2(g) \quad (1)$$

This study concentrates on interactions between gaseous RuO_4 and aluminium, copper and zinc, which can all be found in a BWR

* Corresponding author. Tel.: +46 (0) 31 772 28 03; fax: +46 (0) 31 772 29 31.
E-mail address: joachim.holm@chalmers.se (J. Holm).

0022-3115/$ - see front matter © 2009 Elsevier B.V. All rights reserved.
doi:10.1016/j.jnucmat.2009.03.047

Table 1
Amounts and thicknesses of the metals in the containment at the Forsmark 3 nuclear power plant.

	Amounts (tonnes)	Thickness (μm)	Locations
Aluminium	9	200–5000	Sheets, fans
Copper	2	10[a]	Bars and gratings
Zinc	18	20–70	Floor gratings, ventilation tubes

[a] Assuming copper as aerosol particles.

Fig. 1. The reaction vessel after the completed experiments. Observe the black spots of ruthenium deposits.

containment. A compilation of the amounts of these metals in the Forsmark 3 plant is given in Table 1. Brass is included in this study for a further comparison of copper and zinc. There will probably not be any interactions between brass and RuO_4(g) during a severe accident, since the amounts of brass in the containment can be considered negligible.

A significant deposition of ruthenium was observed on glass during this study, as can be seen in Fig. 1, and the nature of adsorbed ruthenium on these surfaces was investigated as well. Interaction between RuO_4(g) and glass is rather controversial, and some authors [10–12] have reported reactions of RuO_4(g) with glass surfaces at elevated temperatures, 150–300 °C. They proposed reaction (1) as a conceivable process for the sorption mechanism. Others, such as Igarashi et al. [13], have investigated the sorption of ruthenium tetroxide when glass tubes were cooled. Igarashi observed black deposits of ruthenium only when NO or NO_2 was present in the system, and the authorś conclusion was that cooling alone did not cause deposition of gaseous ruthenium tetroxide on the glass surfaces.

2. Experimental

2.1. Production of RuO_4(cr)

RuO_4 can be produced by several methods, using different solvents and oxidizing agents. In the first experiments RuO_4 was distilled by heating a round flask with 5 mg $RuCl_3$ dissolved in minimal amounts of water before adding 5 ml of concentrated H_2SO_4 and 0.25 ml of 0.1 M $KMnO_4$. This method has two major disadvantages, however. First, it is slow at temperatures around 75 °C, which is the optimal temperature for volatilizing RuO_4 [14]. At least 2 h of reaction time were required to reach complete ruthenium distillation. Second, the vapour consists of different by-products, such as manganese, which could be seen as deep purple crystals deposited on the distillation column. In this work, a modification of the method developed by Krtil and Mencl [15] was used. About 50 mg of $RuCl_3$ dissolved in 3 ml of H_2O, 2 ml of 2 M Na_2CO_3 and 0.5 g of $K_2S_2O_8$ were used to distil ruthenium tetroxide. The distillation equipment consisted of a round bottle flask, where the reaction took place, and a glass column. The mixing in the reaction bottle was achieved by a glass-enclosed magnet. An exhaust through a 1 M NaOH trap was connected to the column

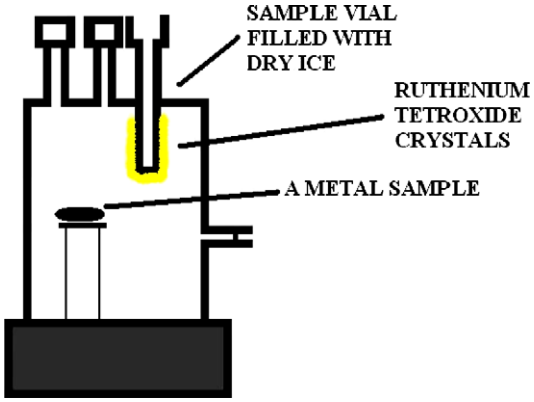

Fig. 2. The experimental set-up for the CVD experiments of RuO_4(g) on aluminium, copper and zinc surfaces.

to prevent RuO_4(g) from escaping. An arbitrary gas flow of oxygen through the system was ensured by connection to a gas tube. The melting point of solid RuO_4 is 27 °C, but it sublimates already at temperatures below 7 °C [16]. Therefore, to keep the crystals in solid form, the RuO_4 vapour formed in the distillation column was allowed to condense on the outer surface of a sample vial filled with dry ice. The sample vial was inserted into the top of the distillation column. About 10 mg of RuO_4(cr) was formed on the vial surface in every batch, and complete ruthenium distillation was reached within 40 min at 75 °C.

2.2. Metal sample preparation

The metals used in almost all experiments were polished discs of aluminium, copper and zinc. The dimensions of the aluminium and copper samples were $10 \times 10 \times 3$ mm (thickness) and the dimensions of the zinc samples were 17 mm (diameter) $\times$ 3 mm (thickness). The samples were prepared before the experiments using a polishing machine with a rotational disc. The grinding paper on the rotational disc was gradually changed during the polishing procedure to less rough paper and was finally exchanged for a polishing cloth and diamond spray. The samples were washed after the polishing procedure in acetone and ethanol in an ultrasound bath. The appearance of the metal sample surfaces at this point was mirror-like.

The metal samples (brass, copper and zinc) used in one experiment were pre-treated in a different way and these samples also had different dimensions, somewhat larger plates with a size of $20 \times 15 \times 1$ mm (thickness). The samples in this experiment were cleaned with diluted sulphuric acid only and were not polished at all.

2.3. Pre-treatment and staining of glass slides

Owing to substantial ruthenium deposits on the glass surfaces in the RuO_4 distillation column and the main experimental set-up (Fig. 2), we decided to examine the nature of adsorbed ruthenium. To do that, glass slides of sodium borosilicate were stained by RuO_4 vapour in the distillation set-up. The slides were placed

Table 2
Experimental conditions for the RuO_4(g) deposition experiments.

Experiment	Metal	Atmosphere	Humidity
1	Zinc	Nitrogen	No
2	Zinc	Air	No
3	Zinc	Nitrogen	Yes
4	Aluminium	Nitrogen	No
5	Aluminium	Air	No
6	Aluminium	Nitrogen	Yes
7	Copper	Nitrogen	No
8	Copper	Air	No
9	Copper	Nitrogen	Yes
T1	Al Zn Cu	Nitrogen	No
T2	Al Zn Cu	Air	No
T3	Al Zn Cu	Nitrogen	Yes
T4	Brass Cu Zn	Air	Yes

approximately 15 cm from the aqueous surface in the distillation column, and the substrate temperature was about room temperature. The glass slides were cleaned with dichromatic acid before staining with RuO_4(g) to ensure a minimum of organic material on the surfaces.

2.4. Experiments on sorption of RuO_4(g) on metal surfaces

Speciation of deposited ruthenium after chemical vapour deposition (CVD) of RuO_4(g) on aluminium, copper and zinc surfaces in different atmospheres was done according to the experiment plan shown in Table 2. The experiments were performed in experimental set-up shown in Fig. 2. The set-up was very simple, consisting of a glass vessel with a special lid equipped with several openings and a simple holder of glass for the metal samples. In the experiments in which three metals were present in the reaction vessel, the metals were attached to special glass hooks, described elsewhere [17].

An experiment was started by placing one or three metals, depending on experiment, on the sample holders. The atmosphere in the system was filled with nitrogen (dry or humid) or air. In the experiments with humid nitrogen atmosphere, the gas was introduced to the system via a gas bubbling bottle. The nitrogen atmosphere in the system was then assumed to be saturated with water vapour, i.e. 100% relative humidity. The ruthenium tetroxide crystals were introduced via the openings of the lid in the set-up, and were allowed to sublimate so pure RuO_4(g) was interacted with the metals. The duration of the experiments was at least 12 h, so all the RuO_4 was sublimated and interacted with the metal samples. The temperature in the set-up during the experiments was room temperature, 22 ± 0.5 °C.

2.5. Desorption of the ruthenium deposits on the metal samples

After CVD with RuO_4(g), all metal samples from experiments T1–T4 were put in a 10 ml solution of 0.2 M NaOH with 5 g/l $K_2S_2O_8$ for 24 h in order to determine the amount of ruthenium on the different metals. This sodium hydroxide solution is reported to be able to dissolve the ruthenium deposits within 24 h [18]. To follow the desorption rate from each metal (aluminium, brass, copper and zinc), 100 µl was taken from four solutions after 1, 5, 30 min, 2, 5, 24, 48 h, 5 days and 1 month after submerging the metals into the solution. The ruthenium content in the remaining samples in series T1–T4 was analyzed 1 month after submersion into the solution. The liquid samples were analyzed for their ruthenium content with inductively coupled plasma–mass spectrometry (ICP–MS).

2.6. Analysis techniques

Several analysis techniques were used in this work to analyze the metal and glass surfaces. The samples were stored under an inert nitrogen atmosphere between the experiments and analyses to prevent changes in the chemical state of the adsorbed ruthenium on the metal samples.

2.6.1. ESCA

Electron spectroscopy for chemical analysis (ESCA) or X-ray photoelectron spectroscopy (XPS) was done using an X-ray spectrophotometer (Perkin Elmer PHI5500 Multi Technique System). This technique is useful for characterizing the speciation of different elements attached to a surface. An ESCA instrument uses an X-ray source to ionize electrons from the surface layer of a solid sample. The energies of these electrons correspond to the bonding energy of the surface electrons attached to the solid sample. The bonding energies of the electrons are characteristic for every element and give information on the chemical bonding, i.e. the chemical state.

2.6.2. SEM

Scanning electron microscopy (SEM) pictures were taken of some of the metal samples after the ESCA measurements. The pictures give information about the degree of surface coverage on the metal samples. The SEM equipment was a LEO 1550 with a GEMINI field emission column.

2.6.3. XRD

X-ray diffraction (XRD) analyses were done to further define the speciation of the ruthenium deposits. The XRD instrument was a Siemens D5000 diffractometer with Cu characteristic radiation, a Göbel mirror on the primary side and long Soler slits with a SOL'X Bruker solid state detector on the secondary side. The instrument has grazing incidence geometry with a 5° fixed incidence angle.

2.6.4. ICP–MS

Inductively coupled plasma–mass spectrometry was used to analyze the amounts of ruthenium in the sodium hydroxide solutions described in Section 2.2. The instrument was an Elan 6000 from Perkin Elmer and the standards were produced by LGC standards.

3. Results and discussion

3.1. CVD of RuO_4 on the metal samples

3.1.1. ESCA measurements

All samples from experiments 1–9 and T1–T3, see Table 2, were analyzed with ESCA. An example of a typical spectrum from the ESCA measurements of an arbitrary metal is shown in Fig. 3. The spectrum shows a magnification of the two main peaks of ruthenium, Ru 3d5/2 and Ru 3d3/2. These two peaks are positioned at binding energies of ~282 and ~286 eV, respectively. However, the spectrum is very complex, and hence six components are necessary to obtain a fit of sufficiently good quality. The two peaks at ~283 and ~287 eV are a high binding energy spin-orbit doublet,

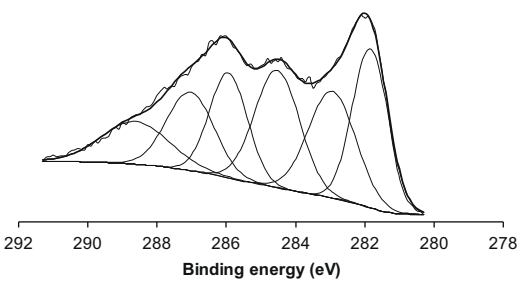

Fig. 3. A typical ESCA spectrum of the two main ruthenium peaks, Ru 3d5/2 and Ru 3d3/2, at binding energies 281.8 and 286.0 eV.

Table 3
Average binding energy of the main ruthenium line Ru 3d5/2 for the three metals.

Metal	Nitrogen	Air	Humid nitrogen	Average	±
Al	281.7	281.5	281.6	281.6	0.1
Cu	281.8	281.9	282.0	281.9	0.1
Zn	281.6	282.1	281.8	281.8	0.3

Table 4
ESCA binding energies (eV) of the Ru 3d5/2 and the O 1s peaks for different ruthenium species.

Reference	[20]	[7]	[21]	[22]	[19]
Ru 3d5/2					
Ru	280.0	280.0	279.9	280.3	
RuO_2	280.7	280.8	282.1	281.0	281.3
$RuO_2 \cdot H_2O$	281.4	282.3			
RuO_3	282.5			282.6	
RuO_4	283.3			283.3	
O 1s[a]					
Lattice oxygen	529.4	529.5		530.0	530.1
Water oxygen	531.5	532.6		531.7	533.5

[a] The oxygen values originate from ESCA measurements of RuO_2 surfaces.

shifted ~1 eV from the main peaks. These high energy binding peaks are formed due to an unscreened final state, described extensively by Rochefort et al. [19]. The two remainder peaks in the spectrum (Fig. 3) originate from two carbon peaks resulting from carbon contamination at 284.5 eV and 288.5 eV. The adaptation of all the peaks in the spectrum is in accordance with ESCA measurements, made by Mun et al. [7], of different ruthenium species.

Table 3 shows the variations in the Ru 3d5/2 binding energy among the three metals in the three different atmospheres used during the experiments. There are no obvious trends in the data, i.e. either the metal substrate or the atmosphere in the experimental set-up has no significant influence on the speciation of the ruthenium deposits. The main ruthenium peak is located around 281.8 ± 0.3 eV for all different conditions and metal samples. The position of the Ru 3d5/2 peak can be compared with binding energies for different ruthenium oxides and compounds reported in the literature; these are shown in Table 4. The position of the Ru 3d5/2 peak (281.8 ± 0.3 eV) in this study is mostly comparable to data reported by Mun et al. [7] (282.3 eV) and Kim and Winograd [20] (281.4 eV), gained in ESCA measurements on hydrous ruthenium dioxide surfaces. RuO_2 is known to behave as a hygroscopic oxide, and the conditions in the reaction bottle were not completely dry even when dry nitrogen was used as the atmosphere. This was primarily due to water on the sample vial with frozen RuO_4(cr).

An attempt was made to confirm the influence of the water content on the ESCA results by heating one of each metal in the series

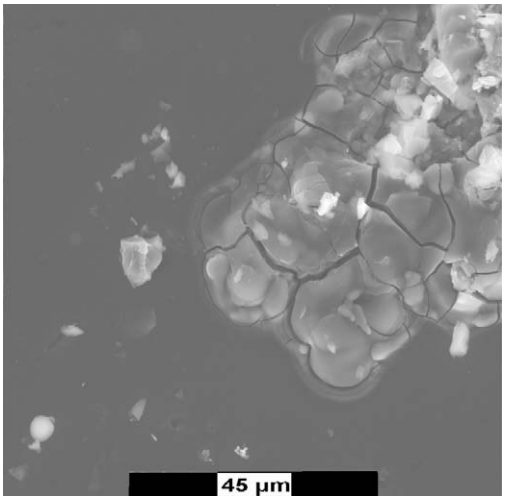

Fig. 5. SEM photograph of an aluminium surface reacted with RuO_4(g).

T1–T3 with deposited ruthenium to 300 °C for a period of 14 h. The heated samples were again analyzed with ESCA but only minor changes at the position of the Ru 3d5/2 peak were observed. However, a comparison was also made of the position of the major oxygen peak O 1s: the spectra are shown in Fig. 4. The oxygen peak O 1s consists of three components, which are attributed to oxygen atoms in three different chemical states (O^{2-}, OH^- and H_2O). These three components are associated with lattice oxygen, hydroxyl groups and water adsorbed on the sample and are positioned in the spectra at BE 529.5, 530.8 and 532.6 eV, respectively. Heating the samples significantly affected the amplitudes of all the peaks in the spectra: the water peaks were almost totally erased, the hydroxyl peak decreased considerably and the lattice oxygen peak became more prominent. These results demonstrate not only the water release from the surface caused by heating the sample; the lattice oxygen in RuO_2 is also more visible in the analyses. The shape of the two spectra in Fig. 4 shows strong similarities with studies of differences between anhydrous and hydrous RuO_2 at ESCA measurements [7,20]. The data from the ESCA analyses imply formation of ruthenium dioxide, hydrous or anhydrous, when ruthenium tetroxide is deposited on metal surfaces.

3.1.2. SEM analyses

The metal samples from experiment series T1, T2 and T3 were investigated with SEM to observe differences in the coverage of RuO_2 on the three metals. Examples of SEM pictures are shown in Figs. 5–7. The pictures indicate less RuO_2 coverage on the aluminium surfaces than on the copper and zinc surfaces and the

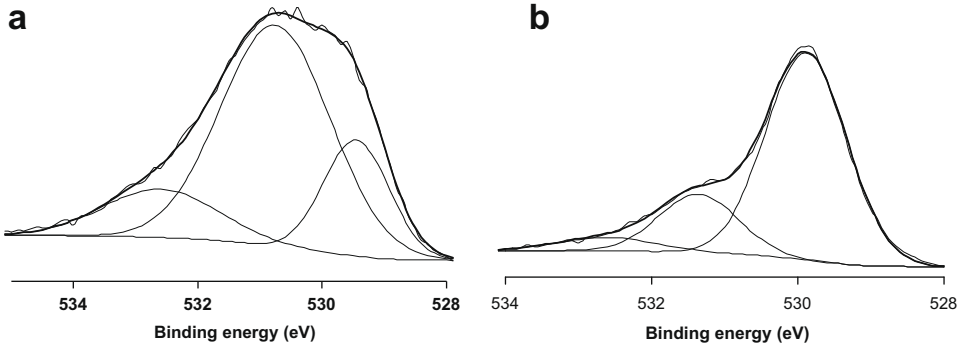

Fig. 4. ESCA spectra of the O 1s peak of (a) an unheated copper sample and (b) a heated copper sample.

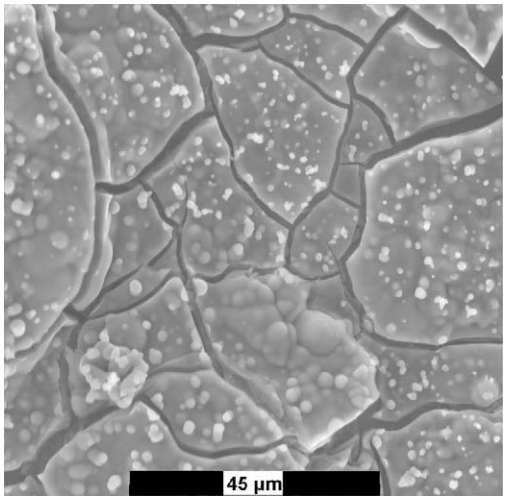

Fig. 6. SEM photograph of a copper surface reacted with RuO_4(g).

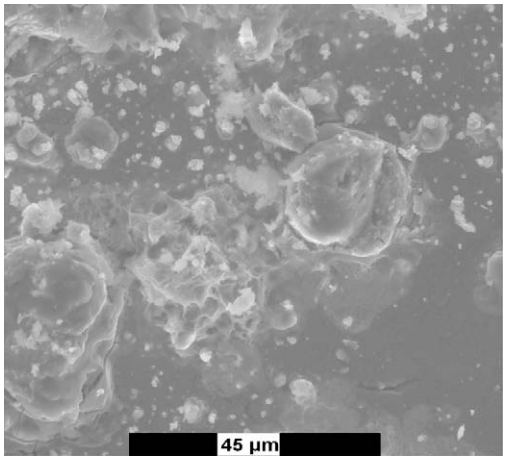

Fig. 7. SEM photograph of a zinc surface reacted with RuO_4(g).

ruthenium layer appeared to be more uniform on the copper surfaces than on the other two metals. The extent of the deposit coverage was further confirmed with observations with the naked eye of the amount of black deposits on the surfaces. The copper and zinc samples had substantial amounts of black deposits on their surfaces while the aluminium pieces showed only spots of black deposits. This is shown in Figs. 8–10.

3.1.3. XRD measurements

An XRD spectrum of one copper sample is shown in Fig. 11. This spectrum shows no traces of the expected ruthenium dioxide on the metal surface. This is also true for the spectra of the aluminium and zinc samples. Difficulties in identifying ruthenium dioxide with XRD on different metals treated with RuO_4(g) have been reported. For example, Mun et al. [18] describe problems in finding any RuO_2 on stainless steel using XRD analysis techniques owing to far too thin RuO_2 layers after CVD treatment with RuO_4(g). This would provide a reasonable explanation of the lack of RuO_2 in the XRD analyses in this study. Another explanation may be the water content in the ruthenium dioxide ($RuO_2 \cdot H_2O$) disturbing the XRD analyses. Sugimoto [23] saw in their XRD analyses of hydrous ruthenium dioxide with different water content that the peak intensity decreased and the peak width widened with increased water content.

Fig. 8. Aluminium samples before and after RuO_4(g) treatment.

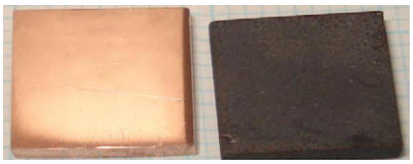

Fig. 9. Copper samples before and after RuO_4(g) treatment.

Fig. 10. Zinc samples before and after RuO_4(g) treatment.

However, a copper-ruthenium compound could be identified on the copper samples analyzed with XRD, samples 9-Cu and T3-Cu – copper(II)-hydroxo-oxoruthenate(VI) ($CuRuO_2(OH)_4$). This copper-ruthenium compound is an orthorhombic compound first discovered by Nowgorocki [24] and later characterized by Hansen [25]. Nowgorocki prepared $CuRuO_2(OH)_4$ by mixing an aqueous solution of potassium perruthenate ($KRuO_4$) with a copper(II) solution, and this resulted in a dark green precipitate of the copper ruthenium compound. The significance of the formation of $CuRuO_2(OH)_4$ on the RuO_4(g) stained copper surfaces in this study is the appearance of a reaction between the copper surfaces and ruthenium tetroxide. The reaction is a dismutation, where copper is oxidized from Cu(0) to Cu(II) and ruthenium is reduced from Ru(VIII) to Ru(VI). However, a similar reaction seems not to have occurred on the RuO_4(g) stained aluminium and zinc samples, since no metal-ruthenium compounds were found in the XRD analyses of these samples.

The dissimilarity of the results with the ESCA and XRD measurements of the RuO_4(g) stained copper samples was unexpected. The $CuRuO_2(OH)_4$ compound is rather unknown [25] and has not been analyzed with the ESCA method, i.e. no ESCA data on $CuRuO_2(OH)_4$ are available. However, the dissimilarity between the two methods might be caused by the difference in thickness of analysed surface layer. The thickness of the analysed layer with ESCA is some nm and for XRD it is some μm. However, the lack of ESCA data for $CuRuO_2(OH)_4$ does not allow any further investigations on the matter.

All samples in series T4 were investigated with XRD, both before and after the CVD with RuO_4(g). The results from the XRD analyses of the metals in series T4 are summarized in Table 5. The pre-analyses of the metal samples were done to identify possible oxide layers on the surfaces, and the analyses confirmed only small amounts of cuprite, Cu_2O, on the copper sample. No oxides were discovered on the brass and zinc samples. No ruthenium compounds were found on the brass and zinc surface in the analyses following the CVD treatment of RuO_4(g) of the samples in the T4 series, although black deposits could be seen with the naked eye. $CuRuO_2(OH)_4$ was discovered again on the copper sample, so

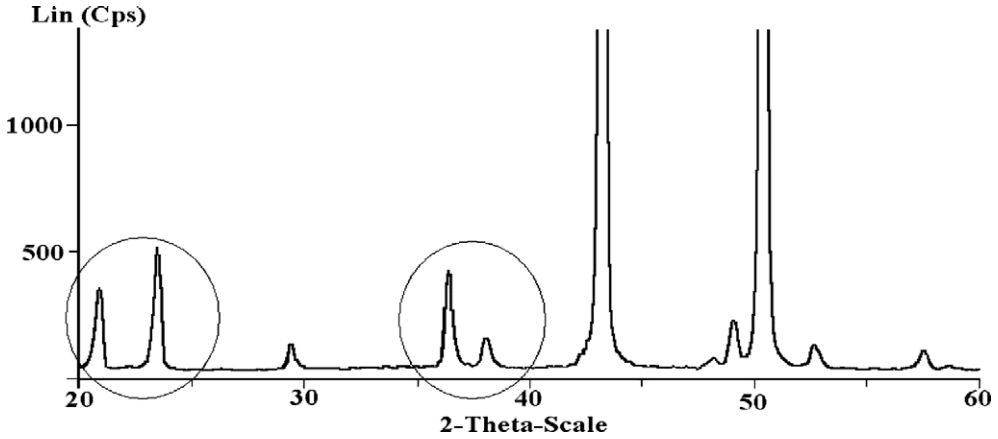

Fig. 11. An XRD spectrum of a copper sample. Observe the peaks inside the two circles, which indicate the $Cu(RuO_2(OH)_4)$ compound on the copper surface.

Table 5
Summary of the surface analyses from the XRD measurements of the metals in series T4.

Metal samples	Before CVD of RuO_4(g)	After CVD of RuO_4(g)	After heat treatment
T4 Brass	Cu and Zn (no oxides)	No ruthenium compounds[a]	RuO_2
T4 Cu	Cu (traces of Cu_2O)	$CuRuO_2(OH)_4$	Traces of RuO_2
T4 Zn	Zn (no oxides)	No ruthenium compounds[a]	RuO_2

[a] Due to screening effects caused by the water content in the ruthenium layer, no RuO_2 was possible to detect with the XRD method.

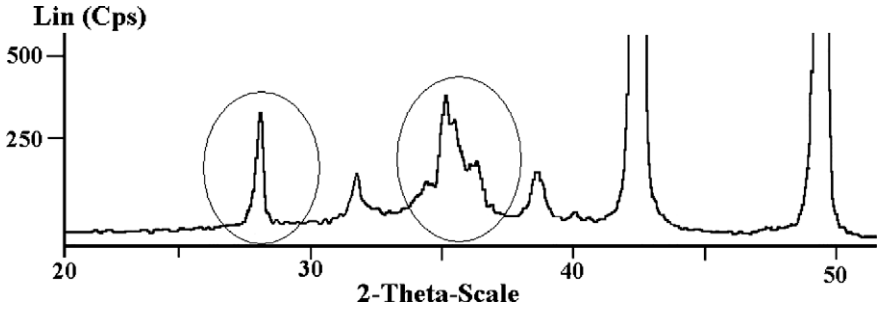

Fig. 12. An XRD spectrum of a heated RuO_4(g) treated brass sample. The two peaks inside the rings mark the RuO_2 peaks.

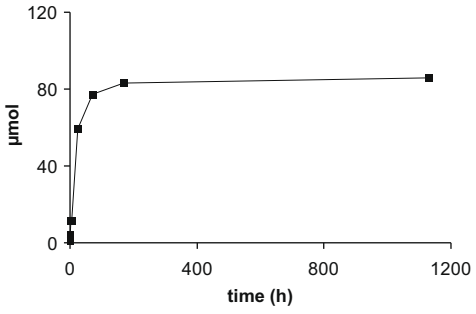

Fig. 13. An example of the desorption rate of the ruthenium deposits from a zinc sample.

the Cu_2O film does not affect the speciation of the ruthenium deposits on the copper surface. After the XRD analysis, these samples were placed in a furnace at 300 °C for 12 h to remove the water in the crystal structure of the expected ruthenium dioxide on the metal samples. RuO_2 was identified (Fig. 12) on the brass and zinc surfaces after heating the metal samples. No $CuRuO_2(OH)_4$ was found on the heated copper sample, but traces of RuO_2 were detected instead. This implies that $CuRuO_2(OH)_4$ is stable and forms only under low temperature conditions.

Table 6
Comparison of amounts of ruthenium on the different metal samples in the T1-T4 series.

Sample	Ruthenium concentration on the metal samples (µmol/cm^2)	Part of total amount deposited ruthenium in each sample series (%)
T1 Al	0.6	3
T1 Cu	3.6	20
T1 Zn	14	77
T2 Al	0.1	3
T2 Cu	0.7	39
T2 Zn	1.0	58
T3 Al	0.1	1
T3 Cu	3.8	59
T3 Zn	2.6	40
T4 Brass	50	70
T4 Cu	11	15
T4 Zn	11	15

3.1.4. ICP–MS measurements

The results of the ICP–MS measurements gave an estimation of the desorption rate of the ruthenium deposits from the metal surfaces. In total, four days were needed to dissolve all the ruthenium deposits from all three metals surfaces, which are illustrated by one of the zinc samples in Fig. 13.

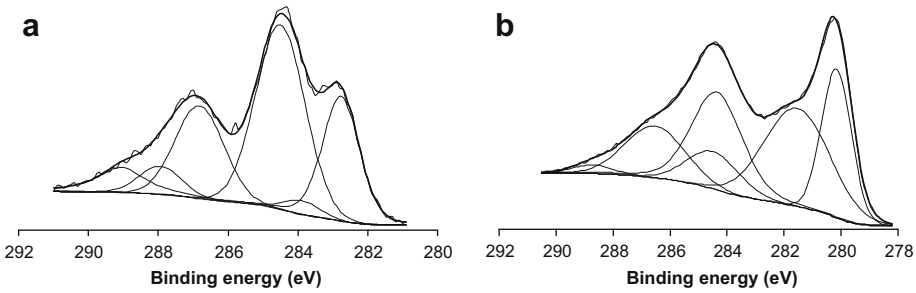

Fig. 14. The ESCA spectra show a significant change of the Ru 3d5/2 binding energy, from 282.8 eV in (a) non heated sample to 280.2 eV in (b) heated sample.

The measurements also showed that ruthenium deposited primarily on the zinc and copper samples in series T1–T3 and mainly on the brass surface in series T4. Table 6 gives the amounts of the ruthenium deposits on the metals in each sample series. The amounts of ruthenium on the copper and zinc metals were at least a factor of six larger than on the aluminium samples. The quantity of ruthenium on the brass surface was almost a factor of five larger than on the copper and zinc surfaces in series T4.

3.2. CVD of RuO_4 on glass samples

The glass slides stained by RuO_4(g) as described in Section 2.5 were covered with thin gray–black deposits of ruthenium after the experiments. The stained glass slides in this work were investigated with ESCA to identify the speciation of ruthenium on the surfaces. The ESCA measurements were made on two glass slides stained by RuO_4(g) but with different post-treatments. The first slide was stored at room temperature and in air; the second glass slide was heated to 300 °C over a period of 14 h in air. The aim of the heating was to remove water from the hydrous ruthenium deposit; as already described, the water in the crystal structure can complicate the ESCA spectra. The two ESCA spectra, with a magnification of the major ruthenium peaks, Ru 3d5/2 and Ru 3d3/2, are shown in Fig. 14. The spectra contain several components to get a fit of high quality. The main ruthenium peak, Ru 3d5/2, in the two spectra is located at apparently differing energy levels, as expected owing to the interfering water content. In the ESCA spectrum of the heated sample, the Ru 3d5/2 peak is located at 280.2 eV, which corresponds to RuO_2 in the literature [26]. The main ruthenium peak in the ESCA spectrum of the non-heated glass sample is located at 282.8 eV, which is a binding energy that is significantly higher than hydrous ruthenium dioxide at 281.4 eV [20]. The binding energy at 282.8 eV for the Ru 3d5/2 peak may indicate that RuO_3 (Table 4) appears on the glass surface. However, the Ru 3d 3/2 peak (286.8 eV) has a significantly lower binding energy than the expected value given in the literature (287.6 eV) [26] for RuO_3. The spin-orbit splitting of the two main ruthenium peaks of the unheated glass sample is thus 4.2 eV, which is more comparable to the spin-orbit splitting of RuO_2 (4.1 eV) than of RuO_3 (4.9 eV) [27]. Furthermore, RuO_3 is known to be an unstable phase [22]. Thus the only reasonable explanation for the high binding energy of Ru 3d5/2 peak in this study was a very high water content in $RuO_2 \cdot H_2O$ on the glass surfaces.

4. Conclusions

Several analysis techniques have been used in this study to characterize and quantify the ruthenium deposits on aluminium, copper, brass, glass and zinc surfaces that were exposed to a vapour of RuO_4. The characterization of the ruthenium deposits detected several ruthenium species on the surfaces: anhydrous ruthenium dioxide, hydrous ruthenium dioxide and copper-hydroxo-oxoruthenate.

The ESCA analyses showed that the ruthenium deposits on the surfaces were similar to data in the literature on hydrous ruthenium dioxide. The hydrous nature of ruthenium dioxide on the surfaces depends not only on the hygroscopic nature of the oxide but also on the humid conditions during the experiments. When the samples were exposed to elevated temperatures, 300 °C, ESCA analysis of the deposits indicated anhydrous ruthenium dioxide.

At least one sample of each RuO_4(g) stained metal used in this work was analyzed with XRD, but RuO_2 was only found on heated (300 °C) metal surfaces. $CuRuO_2(OH)_4$ was found on unheated copper samples stained with RuO_4(g) in the XRD analyses. The detection of $CuRuO_2(OH)_4$ shows that a reaction between the copper surfaces and RuO_4 has occurred and not only a transformation of RuO_4 to RuO_2 on the treated surface. However, when the copper sample was heated to 300 °C only traces of RuO_2 were detected. This implies that $CuRuO_2(OH)_4$ has limited stability at high temperatures.

The grade of deposition on the four metals was investigated with SEM and ICP–MS and the results showed that the deposition of ruthenium was more significant on the brass, copper and zinc surfaces than on the aluminium surfaces. It is consequently probable that the deposition of RuO_4 during a severe accident would appear to a greater extent on copper and zinc surfaces in the reactor containment.

On the basis of the experimental findings in this study, we believe that, in the reactor case, RuO_4(g) released from the nuclear fuel to the containment has the potential to react fast and extensively with the large amount of metal surfaces present there. However, to obtain greater knowledge of the ruthenium-metal interactions in a nuclear containment, studies of the radiolytic effect of revaporisation of deposited ruthenium from the surfaces investigated in this study ought to be performed.

Acknowledgements

This work is funded by the Swedish APRI-6 project, Nordic Nuclear Safety Research (NKS) and Swedish Centre for Nuclear Technology (SKC). The authors are thankful to Vratislav Langer for the XRD analyses and to Urban Jelvestam for assistance with the ESCA analyses.

References

[1] A.L. Wright, Primary System Fission Product Release and Transport. Report NUREG/CR-6193, Oak Ridge National Laboratory, 1994.
[2] J.O. Liljenzin, Personal Communications, Liljenzins Data och Kemikonsult, Göteborg, 2009.
[3] D.A. Powers, L.N. Kmetyk, R.C. Schmidt, A Review of the Technical Issues of Air Ingression during Severe Reactor Accidents. Report NUREG/CR-6218, Sandia National Laboratory, 1994.
[4] C. Mun, L. Cantrel, C. Madic, Nucl. Technol. 156 (2006) 332.
[5] P.W. Cains, S.J. Barnes, J. Nucl. Mater. 186 (1991) 83.
[6] E.D. Maas, J.M. Longo, Nucl. Technol. 47 (1980) 451.

[7] C. Mun, L. Cantrel, C. Madic, Appl. Surf. Sci. 253 (2007) 7613.
[8] B. Eichler, F. Zude, W. Fan, N. Trautman, G. Herrman, Radiochim. Acta 56 (1992) 133.
[9] T. Sakurai, Y. Hinatsu, A. Takahashi, G. Fujisawa, J. Phys. Chem. 89 (1985) 1892.
[10] Z. Yuan, R. Puddephatt, Chem. Mater. 5 (1993) 908.
[11] M. Klein, C. Weyers, W.R.A. Goossens, Volatilisation and Trapping of Ruthenium during Calcination of Nitric Acid Solutions. Technical Report, IAEA-SR-72/03, 1983.
[12] P. Wood, G.H. Bannister, Conference Report, IWGGCR-13: Fission Product Release and Transport in Gas-Cooled Reactors, Berkeley, October 22–25, 1985.
[13] H. Igaraschi, K. Kato, T. Takahashi, Radiochim. Acta 57 (1992) 51.
[14] C. Mun, L. Cantrel, C. Madic, in: Nuclear Energy for New Europe 2005, Bled, Slovenia, 2005.
[15] J. Krtil, J. Mencl, Radiochem. Radioanal. Lett. 7 (1971) 175.
[16] G.E. Runkle, J. Aerosol. Sci. 10 (1979) 431.
[17] H. Glänneskog, Y. Albinsson, J.O. Liljenzin, G. Skarnemark, Nucl. Instrum. and Meth. B 498 (2003) 517.
[18] C. Mun, L. Cantrel, C. Madic, Radiochim. Acta 95 (2007) 643.
[19] D. Rochefort, P. Dabo, D. Guay, P.M.A. Sherwood, Electrochim. Acta 48 (2003) 4245.
[20] K.S. Kim, N. Winograd, J. Catal. 35 (1974) 66.
[21] B. Folkesson, Acta Chem. Scand. 27 (1973) 287.
[22] H.Y.H. Chan, C.G. Takoudis, M.J. Weaver, J. Catal. 172 (1997) 336.
[23] W. Sugimoto, J. Phys. Chem. 109 (2005) 7330.
[24] G. Nowgorocki, Thèse, Université Lille, 1967.
[25] T. Hansen, Mater. Sci. Forum 228–231 (1996) 723.
[26] D. Briggs, M.P. Seah, Practical Surface Analysis, Auger and X-ray Photoelectron Spectroscopy, 2nd Ed., vol. 1, Wiley Interscience, 1990.
[27] A. Iembo, F. Fuso, E. Arimondo, C. Ciofi, G. Pennelli, G.M. Curro, F. Neri, M. Allegrini, J. Mater. Res. 12 (1997) 1433.